Int. J. Solids Structures, 1966, Vol. 2, pp. 307 to 318. Pergamon Press Ltd. Printed in Great Britain

ON THE ANALYSIS OF TRIANGULAR MESH GRILLAGES

J. D. RENTON

Department of Engineering Science, University of Oxford, Oxford, England

Abstract—Finite difference equations for the analysis of triangular mesh grillages are derived on the assumption that the torsional stiffnesses of the individual beams are negligible. General solutions of these equations are given and can be used as a rapid means of finding the deflections of such grillages. These solutions are applied to give the deflections of grillages with rectangular, circular and triangular boundaries. In the particular cases examined it is shown that, as the mesh becomes infinitely fine, the grillages tend to behave like plates.

NOTATION

a	length of a grillage beam
D	$3\sqrt{(3)}EI/4a$
EI	bending stiffness of a grillage beam
E_x, E_y	finite difference operators defined by equations (8) and (9)
F	shearing force applied to the end of a beam
GJ	torsional stiffness of a beam
K_1 to K_7	constants defined by equations (15) to (21)
M	bending moment
q	distributed load per unit area
M_ξ, M_η	clockwise moments about the axes ξ and η respectively
T	torsional moment
W	load applied normal to the grillage at a joint
x, y	oblique finite difference co-ordinates shown in Fig. 2
X, Y	Cartesian co-ordinates parallel to the axes η and ξ respectively
α	$2EI/a^3$
β	GJ/a
γ	angle between the axis of a beam and the axis ξ (see Fig. 1)
$\delta_{i,j}$	Kronecker delta
$\delta(x, y)$	deflection of a joint with co-ordinates (x, y)
θ_ξ, θ_η	clockwise rotations about the axes ξ and η respectively
μ, ν	constants
ξ, η	finite difference co-ordinates as shown in Fig. 2
ϕ	bending rotation of a beam as shown in Fig. 1
ψ	torsional rotation of a beam as shown in Fig. 1
ω	joint displacement normal to the plane of the grillage beams

The subscripts 1 and 2 refer to the ends 1 and 2 of the beam shown in Fig. 1.

1. INTRODUCTION

FINITE difference calculus has already been used to analyse the behaviour of rectangular mesh grillages. By this method, Ellington and McCallion [1] have derived the moments and deflections induced in such grillages, on the assumption that the torsional stiffnesses of the members are negligible. Thein Wah [2] has extended this analysis to allow for the torsional stiffnesses of the members and obtained solutions by methods analogous to those used by Navier and Levy for plate problems. The author [3], also allowing for the torsional stiffnesses of the members, has suggested a more general form of Navier solution, using a double Fourier series, and given other solutions for circular boundary conditions. Similar methods can be applied to the analysis of triangular mesh grillages if an oblique co-ordinate system is used. A large proportion of such grillages have equilateral triangular meshes and attention will be confined to such cases, although the method could also be applied to other forms of triangular mesh provided that the forms are generated by repetition of a basic pattern of members.

2. THE DIFFERENCE EQUATIONS

The ordinary slope-deflection equations, relating the loads and deflections at the ends of a beam, may be written in the following matrix form

$$\begin{bmatrix} T_1 \\ M_1 \\ F_1 \end{bmatrix} = \begin{bmatrix} \beta & 0 & 0 \\ 0 & 2a^2\alpha & 3a\alpha \\ 0 & 3a\alpha & 6\alpha \end{bmatrix} \begin{bmatrix} \psi_1 \\ \phi_1 \\ \omega_1 \end{bmatrix} + \begin{bmatrix} -\beta_1 & 0 & 0 \\ 0 & a^2\alpha & -3a\alpha \\ 0 & 3a\alpha & -6\alpha \end{bmatrix} \begin{bmatrix} \psi_2 \\ \phi_2 \\ \omega_2 \end{bmatrix} \tag{1}$$

$$\begin{bmatrix} T_2 \\ M_2 \\ F_2 \end{bmatrix} = \begin{bmatrix} -\beta & 0 & 0 \\ 0 & a^2\alpha & 3a\alpha \\ 0 & -3a\alpha & -6\alpha \end{bmatrix} \begin{bmatrix} \psi_1 \\ \phi_1 \\ \omega_1 \end{bmatrix} + \begin{bmatrix} \beta & 0 & 0 \\ 0 & 2a^2\alpha & -3a\alpha \\ 0 & -3a\alpha & 6\alpha \end{bmatrix} \begin{bmatrix} \psi_2 \\ \phi_2 \\ \omega_2 \end{bmatrix} \tag{2}$$

where

$$\alpha = 2EI/a^3, \qquad \beta = GJ/a \tag{3}$$

and, as shown in Fig. 1, the subscripts 1 and 2 refer to the ends 1 and 2 of a beam of length a, T is a torque, M a bending moment, F a shearing force, ψ an angle of twist, ϕ an angle of bending and ω a vertical displacement. The bending stiffness of the beam is EI and its torsional stiffness is GJ.

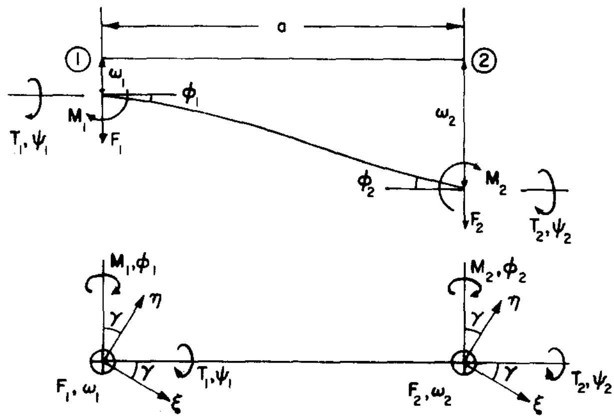

FIG. 1.

If these stiffness matrices are referred to co-ordinates ξ, η inclined at a clockwise angle γ to the original system, as shown in Fig. 1, then the stiffness matrices of equations

(1) and (2) must be premultiplied by a matrix t and post-multiplied by its transpose where

$$t = \begin{bmatrix} \cos\gamma & -\sin\gamma & 0 \\ \sin\gamma & \cos\gamma & 0 \\ 0 & 0 & 1 \end{bmatrix} \tag{4}$$

giving

$$\begin{bmatrix} M_{\xi 1} \\ M_{\eta 1} \\ F_1 \end{bmatrix} = \begin{bmatrix} \beta\cos^2\gamma + 2a^2\alpha\sin^2\gamma & \sin\gamma\cos\gamma(\beta - 2a^2\alpha) & -3a\alpha\sin\gamma \\ \sin\gamma\cos\gamma(\beta - 2a^2\alpha) & \beta\sin^2\gamma + 2a^2\alpha\cos^2\gamma & 3a\alpha\cos\gamma \\ -3a\alpha\sin\gamma & 3a\alpha\cos\gamma & 6\alpha \end{bmatrix} \begin{bmatrix} \theta_{\xi 1} \\ \theta_{\eta 1} \\ \omega_1 \end{bmatrix}$$
$$+ \begin{bmatrix} -\beta\cos^2\gamma + a^2\alpha\sin^2\gamma & \sin\gamma\cos\gamma(-\beta - a^2\alpha) & 3a\alpha\sin\gamma \\ \sin\gamma\cos\gamma(-\beta - a^2\alpha) & -\beta\sin^2\gamma + a^2\alpha\cos^2\gamma & -3a\alpha\cos\gamma \\ -3a\alpha\sin\gamma & 3a\alpha\cos\gamma & -6\alpha \end{bmatrix} \begin{bmatrix} \theta_{\xi 2} \\ \theta_{\eta 2} \\ \omega_2 \end{bmatrix} \tag{5}$$

$$\begin{bmatrix} M_{\xi 2} \\ M_{\eta 2} \\ F_2 \end{bmatrix} = \begin{bmatrix} -\beta\cos^2\gamma + a^2\alpha\sin^2\gamma & \sin\gamma\cos\gamma(-\beta - a^2\alpha) & -3a\alpha\sin\gamma \\ \sin\gamma\cos\gamma(-\beta - a^2\alpha) & -\beta\sin^2\gamma + a^2\alpha\cos^2\gamma & 3a\alpha\cos\gamma \\ 3a\alpha\sin\gamma & -3a\alpha\cos\gamma & -6\alpha \end{bmatrix} \begin{bmatrix} \theta_{\xi 1} \\ \theta_{\eta 1} \\ \omega_1 \end{bmatrix}$$
$$+ \begin{bmatrix} \beta\cos^2\gamma + 2a^2\alpha\sin^2\gamma & \sin\gamma\cos\gamma(\beta - 2a^2\alpha) & 3a\alpha\sin\gamma \\ \sin\gamma\cos\gamma(\beta - 2a^2\alpha) & \beta\sin^2\gamma + 2a^2\alpha\cos^2\gamma & -3a\alpha\cos\gamma \\ 3a\alpha\sin\gamma & -3a\alpha\cos\gamma & 6\alpha \end{bmatrix} \begin{bmatrix} \theta_{\xi 2} \\ \theta_{\eta 2} \\ \omega_2 \end{bmatrix} \tag{6}$$

Using equations (5) and (6), the loads applied at any joint of the grillage can be expressed in terms of the deflections of that joint and of the adjacent joints. Two systems of finite difference co-ordinates (x, y) and (ξ, η) will be used, where

$$\xi = x + y, \qquad \eta = x - y. \tag{7}$$

Figure 2 shows the co-ordinates of a general joint and the adjacent joints of the grillage in terms of both systems. The deflections of the adjacent joints may be expressed in terms

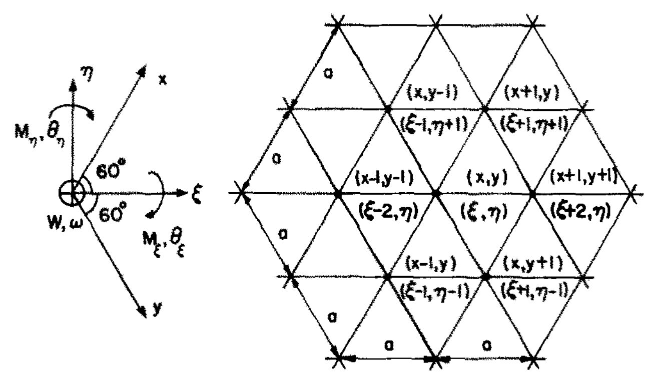

FIG. 2.

of the deflections of the joint (x, y) by means of finite difference operators E_x and E_y where

$$E_x\delta(x, y) = \delta(x+1, y); \qquad E_x\delta(\xi, \eta) = \delta(\xi+1, \eta+1) \tag{8}$$

$$E_y\delta(x, y) = \delta(x, y+1); \qquad E_y\delta(\xi, \eta) = \delta(\xi+1, \eta-1) \tag{9}$$

and $\delta(x, y)$, for example, is the deflection of the joint (x, y). If the torsional stiffness of the grillage beams are taken as negligible in comparison with their bending stiffnesses, then the external loads M_ξ, M_η and W applied at the joint (x, y) are expressed by

$$\frac{4M_\xi}{\sqrt{(3)}a^2\alpha} = [(E_x^{-1}+E_y^{-1})+(E_x+E_y)+8]\sqrt{(3)}\theta_\xi - [(E_x^{-1}-E_y^{-1})+(E_x-E_y)]\theta_\eta$$

$$-6[(E_x^{-1}-E_y^{-1})-(E_x-E_y)]\frac{\omega}{a} \tag{10}$$

$$\frac{4M_\eta}{a^2\alpha} = -[(E_x^{-1}-E_y^{-1})+(E_x-E_y)]\sqrt{(3)}\theta_\xi + [(E_x^{-1}+E_y^{-1})+(E_x+E_y)+4(E_x^{-1}E_y^{-1}+E_xE_y)$$

$$+24]\theta_\eta + 6[(E_x^{-1}+E_y^{-1})-(E_x+E_y)+2(E_x^{-1}E_y^{-1}-E_xE_y)]\frac{\omega}{a} \tag{11}$$

$$\frac{2W}{3a\alpha} = [(E_x^{-1}-E_y^{-1})-(E_x-E_y)]\sqrt{(3)}\theta_\xi - [(E_x^{-1}+E_y^{-1})-(E_x+E_y)+2(E_x^{-1}E_y^{-1}-E_xE_y)]\theta_\eta$$

$$-4[(E_x^{-1}+E_y^{-1})+(E_x+E_y)+(E_x^{-1}E_y^{-1}+E_xE_y)-6]\frac{\omega}{a}. \tag{12}$$

It will be seen that equations (10) to (12) could have been written in a symmetrical matrix form in accordance with Clerk Maxwell's reciprocal theorem.

3. SOLUTION OF THE DIFFERENCE EQUATIONS

For convenience, all solutions will be expressed in terms of the co-ordinates (ξ, η) rather than the co-ordinates (x, y). It has been shown [3] that if

$$\mathfrak{E}\{f(\xi, \eta)\} = g(\xi, \eta) \tag{13}$$

where $\mathfrak{E}\{f(\xi, \eta)\}$ is any finite difference function of the function $f(\xi, \eta)$ in terms of the operators E_x and E_y and $g(\xi, \eta)$ is the resulting function then

$$\mathfrak{E}\{\mathfrak{D}[f(\xi, \eta)]\} = \mathfrak{D}[\mathfrak{E}\{f(\xi, \eta)\}] = \mathfrak{D}[g(\xi, \eta)] \tag{14}$$

where $\mathfrak{D}[f(\xi, \eta)]$ is any partial differential function of the function $f(\xi, \eta)$ Thus, having established relationships of the type given by equation (13), further relationships can be found by using equation (14). For example, the following Table 1 lists functions $f(\xi, \eta)$ in the left hand column. A finite difference function $\mathfrak{E}$ is listed at the head of each column and the results $g(\xi, \eta)$ of its operation on the functions $f(\xi, \eta)$ are listed below it.

TABLE 1

	$(E_x^{-1}+E_y^{-1})+(E_x+E_y)$	$(E_x^{-1}-E_y^{-1})+(E_x-E_y)$	$E_x^{-1}E_y^{-1}+E_xE_y$
ξ^5	$4(\xi^5+10\xi^3+5\xi)$	0	$2(\xi^5+40\xi^3+80\xi)$
η^5	$4(\eta^5+10\eta^3+5\eta)$	0	$2\eta^5$
$\xi^4\eta^4$	$4(\xi^4+6\xi^2+1)(\eta^4+6\eta^2+1)$	$64(\xi^3\eta^3+\xi^3\eta+\xi\eta^3+\xi\eta)$	$2\eta^4(\xi^4+24\xi^2+16)$
$\cos\mu\xi\cos\nu\eta$	$4\cos\mu\cos\nu\cos\mu\xi\cos\nu\eta$	$4\sin\mu\sin\nu\sin\mu\xi\sin\nu\eta$	$2\cos 2\mu\cos\mu\xi\cos\nu\eta$
	$(E_x^{-1}+E_y^{-1})-(E_x+E_y)$	$(E_x^{-1}-E_y^{-1})-(E_x-E_y)$	$E_x^{-1}E_y^{-1}-E_xE_y$
ξ^5	$-4(5\xi^4+10\xi^2+1)$	0	$-4(5\xi^4+40\xi^2+16)$
η^5	0	$-4(5\eta^4+10\eta^2+1)$	0
$\xi^4\eta^4$	$-16(\xi^3+\xi)(\eta^4+6\eta^2+1)$	$-16(\eta^3+\eta)(\xi^4+6\xi^2+1)$	$-16\eta^4(\xi^3+4\xi)$
$\cos\mu\xi\cos\nu\eta$	$4\sin\mu\cos\nu\sin\mu\xi\cos\nu\eta$	$4\cos\mu\sin\nu\cos\mu\xi\sin\nu\eta$	$2\sin 2\mu\sin\mu\xi\cos\nu\eta$

The result of any operation on any function considered in this paper can now be obtained from Table 1 by using equation (14). For example

$$[(E_x^{-1}-E_y^{-1})+(E_x-E_y)]\{\xi^3\eta^2\} = [(E_x^{-1}-E_y^{-1})+(E_x-E_y)]\left\{\frac{1}{48}\frac{\partial}{\partial\xi}\frac{\partial^2}{\partial\eta^2}[\xi^4\eta^4]\right\}$$
$$= \frac{1}{48}\frac{\partial}{\partial\xi}\frac{\partial^2}{\partial\eta^2}[64(\xi^3\eta^3+\xi^3\eta+\xi\eta^3+\xi\eta)] = 8(3\xi^2\eta+\eta).$$

On substituting functions obtained in this way into equations (10) to (12), solutions for various loading conditions can be found. The most common problems concern the behaviour of grillages when only forces normal to the grillage are acting, so that M_ξ and M_η will be taken as zero. The fundamental solutions for such cases are given in the following table, where the related deflection or load functions appear on the same line below the appropriate deflection or load.

TABLE 2

θ_ξ	θ_η	ω	W
0	$(30\xi^4-44)/3a$	ξ^5	$1080\alpha\xi$
$(-30\eta^4+4)/3\sqrt{(3)}a$	0	η^5	$120\alpha\eta$
$\dfrac{8(-9\xi^4\eta^3+6\eta^3+36\xi^2\eta-14\eta)}{9\sqrt{(3)}a}$	$\dfrac{8(27\xi^3\eta^4-6\xi^3-36\xi\eta^2+34\xi)}{27a}$	$\xi^4\eta^4$	$24\alpha(\xi^4+36\xi^2\eta^2+9\eta^4+\frac{5}{27})$
0	$K_1\sin\mu\xi$	$\cos\mu\xi$	$K_2\cos\mu\xi$
$K_3\sin\nu\eta$	0	$\cos\nu\eta$	$K_4\cos\nu\eta$
$K_5\cos\mu\xi\sin\nu\eta$	$K_6\sin\mu\xi\cos\nu\eta$	$\cos\mu\xi\cos\nu\eta$	$K_7\cos\mu\xi\cos\nu\eta$

where

$$K_1 = -\frac{6}{a}\left[\frac{\sin\mu+\sin 2\mu}{2\cos 2\mu+\cos\mu+6}\right] \tag{15}$$

$$K_2 = -12\alpha\left[\cos 2\mu+2\cos\mu-3+\frac{3(\sin\mu+\sin 2\mu)^2}{2\cos 2\mu+\cos\mu+6}\right] \tag{16}$$

$$K_3 = \frac{2\sqrt{(3)}\sin\nu}{a(\cos\nu+2)} \tag{17}$$

$$K_4 = 12\alpha\left[\frac{(1-\cos\nu)^2}{\cos\nu+2}\right] \tag{18}$$

$$K_5 = \frac{2\sqrt{3}}{a}\left[\frac{\sin\nu(2\cos^3\mu+6\cos\mu+\cos\nu)}{4\cos^3\mu\cos\nu+9\cos^2\mu+\cos^2\nu+6\cos\mu\cos\nu+7}\right] \tag{19}$$

$$K_6 = -\frac{6}{a}\left[\frac{\sin\mu(2\cos^2\mu\cos\nu+5\cos\mu+2\cos\nu)}{4\cos^3\mu\cos\nu+9\cos^2\mu+\cos^2\nu+6\cos\mu\cos\nu+7}\right] \tag{20}$$

$$K_7 = -12\alpha\left[\cos 2\mu+2\cos\mu\cos\nu-3+\frac{\sqrt{(3)}a}{2}K_5\cos\mu\sin\nu -\frac{a}{2}K_6\sin\mu(2\cos\mu+\cos\nu)\right]. \tag{21}$$

Further solutions can again be established by means of equation (14) and also by substituting imaginary or even complex values for μ and ν. Examples of the application of these solutions to specific loading and boundary conditions will now be examined.

4. RECTANGULAR BOUNDARY PROBLEMS

It has previously been shown [3] that any loading on a rectangular mesh grillage may be represented by a double Fourier type of series. The same is true of a triangular mesh grillage and the appropriate expansion in this case is

$$W = W(\xi,\eta) = \sum_{s=0}^{q}\sum_{r=0}^{p}\left(a_{sr}\cos\frac{2\pi s}{m}\xi\cos\frac{2\pi r}{n}\eta+b_{sr}\cos\frac{2\pi s}{m}\xi\sin\frac{2\pi r}{n}\eta + c_{sr}\sin\frac{2\pi s}{m}\xi\cos\frac{2\pi r}{n}\eta+d_{sr}\sin\frac{2\pi s}{m}\xi\sin\frac{2\pi r}{n}\eta\right) \tag{22}$$

where

$$a_{sr} = \sum_{\xi=0}^{m-1}\sum_{\eta=1}^{n-1}\frac{4W(\xi,\eta)\cos(2\pi s/m)\xi\cos(2\pi r/n)\eta}{mn(1+\delta_{s,0})(1+\delta_{2s,m})(1+\delta_{r,0})(1+\delta_{2r,n})} \tag{23}$$

$$b_{sr} = \sum_{\xi=0}^{m-1}\sum_{\eta=1}^{n-1}\frac{4W(\xi,\eta)\cos(2\pi s/m)\xi\sin(2\pi r/n)\eta}{mn(1+\delta_{s,0})(1+\delta_{2s,m})} \tag{24}$$

$$c_{sr} = \sum_{\xi=1}^{m-1}\sum_{\eta=0}^{n-1}\frac{4W(\xi,\eta)\sin(2\pi s/m)\xi\cos(2\pi r/n)\eta}{mn(1+\delta_{r,0})(1+\delta_{2r,n})} \tag{25}$$

$$d_{sr} = \sum_{\xi=1}^{m-1}\sum_{\eta=1}^{n-1}\frac{4W(\xi,\eta)}{mn}\sin\frac{2\pi s}{m}\xi\sin\frac{2\pi r}{n}\eta \tag{26}$$

and $\delta_{i,j}$ is a Kronecker delta. For any values of $2q$ and $2p$ less than m and n, respectively, equations (22) to (26) give the best representation of any generalized loading $W(\xi, \eta)$ in terms of a double Fourier type of series in the range of integer values of ξ between the limits 0 and $m-1$ and integer values of η between 0 and $n-1$.

A particular problem of interest is the analysis of a triangular mesh grillage with a pinned rectangular boundary. In this case it is more convenient to express the loading entirely in terms of sine functions even though, for a given number of terms, the accuracy of the expansion may be reduced. For the case of rectangular mesh grillages, the resulting Navier type of solution has already been given by Thein Wah [2]. The expression for the loading now reduces to the form

$$W = \sum_{s=1}^{m-1} \sum_{r=1}^{n-1} d'_{sr} \sin \frac{\pi s}{m} \xi \sin \frac{\pi r}{n} \eta \tag{27}$$

where

$$d'_{sr} = \sum_{\xi=1}^{m-1} \sum_{\eta=1}^{n-1} \frac{4W(\xi, \eta)}{mn} \sin \frac{\pi s}{m} \xi \sin \frac{\pi r}{n} \eta \tag{28}$$

and the boundaries lie on ξ equal to 0 or m, η equal to 0 or n. Then from Table 2 it can be deduced that the deflections of a joint with co-ordinates (ξ, η) are given by

$$\theta_\xi = \sum_{s=1}^{m-1} \sum_{r=1}^{n-1} -d'_{sr} \frac{K_5}{K_7} \sin \frac{\pi s}{m} \xi \cos \frac{\pi r}{n} \eta \tag{29}$$

$$\theta_\eta = \sum_{s=1}^{m-1} \sum_{r=1}^{n-1} -d'_{sr} \frac{K_6}{K_7} \cos \frac{\pi s}{m} \xi \sin \frac{\pi r}{n} \eta \tag{30}$$

$$\omega = \sum_{s=1}^{m-1} \sum_{r=1}^{n-1} \frac{d'_{sr}}{K_7} \sin \frac{\pi s}{m} \xi \sin \frac{\pi r}{n} \eta . \tag{31}$$

It follows directly that the boundary conditions of zero displacement and zero rotation about an axis normal to the boundary are fully satisfied. Since the functions used are skew symmetrical about the boundaries, the condition, that no moments are applied about the boundaries, is also satisfied.

5. CLAMPED CIRCULAR BOUNDARIES

The equation of a circle of radius R in terms of the co-ordinates (ξ, η) is given by

$$\xi^2 + 3\eta^2 - \frac{4R^2}{a^2} = 0 \tag{32}$$

As previously noted [3], only integer values of ξ and η are completely meaningful so that the above equation really represents a number of discrete points at which the joints of the grillage coincide with the circle. However, it is convenient and sufficiently accurate for most purposes to consider the equation to apply to all points at which the grillage meets the circle. It was found [3] that the maximum error involved in such an assumption, when applied to a rectangular grillage with a circular boundary of fourteen bays diameter, was 2·7 per cent of the central deflection.

Choosing suitable derivatives of the solutions given on the first three lines of Table 2, the following solution gives the deflections induced by a uniform load W applied to each joint of a triangular mesh grillage with a clamped circular boundary.

$$\theta_\xi = \frac{-W\eta}{24\sqrt{(3)}a\alpha}\left(\xi^2+3\eta^2-\frac{4R^2}{a^2}\right) \tag{33}$$

$$\theta_\eta = \frac{W\xi}{72a\alpha}\left(\xi^2+3\eta^2-\frac{4R^2}{a^2}\right) \tag{34}$$

$$\omega = \frac{W}{576\alpha}\left(\xi^2+3\eta^2-\frac{4R^2}{a^2}\right)^2. \tag{35}$$

It will be observed that the conditions of zero displacement and rotation on the boundary are fully satisfied.

6. PINNED TRIANGULAR BOUNDARIES

Figure 3 shows a triangular mesh grillage with a triangular boundary. If the length of a perpendicular from a vertex to a side of the boundary is A and the origin of co-ordinates

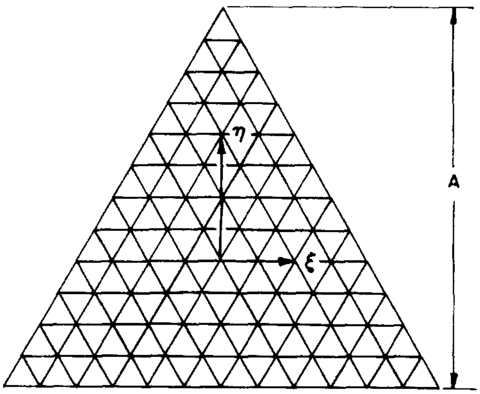

FIG. 3.

is taken at the centroid of this triangle then the equations of the three boundaries are

$$\eta = -\frac{2A}{3\sqrt{(3)}a}; \qquad \xi+\eta = \frac{4A}{3\sqrt{(3)}a}; \qquad \xi-\eta = \frac{-4A}{3\sqrt{(3)}a} \tag{36}$$

The most general fifth-order expression for ω, giving zero vertical displacement on these boundaries and which is also cyclically symmetrical with regard to a rotation through 120° about the centroid, is

$$\begin{aligned}\omega &= C\left(\eta+\frac{2A}{3\sqrt{(3)}a}\right)\left(\xi+\eta-\frac{4A}{3\sqrt{(3)}a}\right)\left(\xi-\eta+\frac{4A}{3\sqrt{(3)}a}\right)\left(\xi^2+3\eta^2-b^2\right)\\ &= -C\left[\eta^3-\xi^2\eta-\frac{2A}{3\sqrt{(3)}a}(\xi^2+3\eta^2)+\frac{32A^3}{81\sqrt{(3)}a^3}\right][\xi^2+3\eta^2-b^2]\end{aligned} \tag{37}$$

where b and C are constants. The corresponding expressions for θ_ξ and θ_η are

$$\theta_\xi = -\frac{2C}{\sqrt{(3)}a}\left[\xi^4+6\xi^2\eta^2-15\eta^4+\frac{8A}{\sqrt{(3)}a}\eta(\xi^2+3\eta^2)-b^2(\xi^2-3\eta^2)-\frac{4A}{\sqrt{(3)}a}\eta\left(b^2+\frac{16A^2}{27a^2}\right)\right] \tag{38}$$

$$\theta_\eta = \frac{4C}{3a}\left[\eta+\frac{2A}{3\sqrt{(3)}a}\right]\left[6\xi^2+6\eta^2+\frac{8A}{\sqrt{(3)}a}-\frac{16A^2}{9a^2}-3b^2\right]. \tag{39}$$

Obviously, θ_η is zero on the first boundary given by equations (36) so that there is no rotation about an axis perpendicular to this boundary. Then since the solution is cyclically symmetrical with respect to a rotation through 120°, it follows that boundary rotations are confined to rotations about the boundary lines as would normally be the case for pinned supports.

By the same methods as those used to derive the original equations, it is possible to establish that the moment applied about a boundary parallel to the ξ axis, M_ξ^B say, is given by

$$\frac{4M_\xi^B}{\sqrt{(3)}a^2\alpha} = [E_x+E_y^{-1}+4]\sqrt{(3)}\theta_\xi-[-E_y^{-1}+E_x]\theta_\eta-6[-E_y^{-1}-E_x+2]\frac{\omega}{a} \tag{40}$$

Attention has already been confined to cases where M_ξ is zero at all joints of the grillage. Further, if M_ξ^B is zero at a boundary on which ω is also zero, then from equations (10) and (40) it follows that

$$[(E_x^{-1}-E_y^{-1})-(E_x-E_y)]\sqrt{(3)}\theta_\xi-[(E_x^{-1}+E_y^{-1})-(E_x+E_y)]\theta_\eta$$
$$-6[(E_x^{-1}+E_y^{-1})+(E_x+E_y)]\frac{\omega}{a} = 0. \tag{41}$$

The form of equation (41) is more convenient to use than that obtained by equating the right-hand side of equation (40) to zero since in the former case Table 1 can be used. On substituting the deflections given by equations (37) to (39) into equation (41) it will be found that the moment about the boundary, given by the first of equations (36), is zero if

$$b^2 = 4\left(\frac{4A^2}{9a^2}-1\right). \tag{42}$$

Again, from the cyclic symmetry of the solution chosen, the bending moments about the other boundaries are also zero for the same value of b. Thus the full and exact solution for a triangular mesh grillage with triangular pinned boundaries, of the type shown in Fig. 3, loaded by a uniform load W at each joint is given by

$$\theta_\xi = \frac{-W}{192A\alpha}\left[\left(\xi^2+3\eta^2+\frac{4A\eta}{\sqrt{(3)}a}\right)^2-24\eta^4-12\eta^2-4\left(\frac{4A^2}{9a^2}-1\right)\left(\xi^2+\frac{16A\eta}{3\sqrt{(3)}a}\right)-\frac{16A\eta}{3\sqrt{(3)}a}\right] \tag{43}$$

$$\theta_\eta = \frac{\sqrt{(3)}W\xi}{48A\alpha}\left[\eta+\frac{2A}{3\sqrt{(3)}a}\right]\left[\xi^2+\eta^2+\frac{4A\eta}{3\sqrt{(3)}a}-\frac{32A^2}{27a^2}+2\right] \tag{44}$$

$$\omega = \frac{\sqrt{(3)}Wa}{384A\alpha}\left[\eta^3-\xi^2\eta-\frac{2A}{3\sqrt{(3)}a}(\xi^2+3\eta^2)+\frac{32A^3}{81\sqrt{(3)}a^3}\right]\left[\frac{16A^2}{9a^2}-4-\xi^2-3\eta^2\right]. \tag{45}$$

7. THE PLATE ANALOGY

When the mesh of the grillage becomes very fine, that is to say when the bay length a is very small in comparison with the overall dimensions of the grillage, the plate-like behaviour of the grillage becomes more apparent. To examine this, it is convenient to introduce a new co-ordinate system (X, Y) related to the physical dimensions of the grillage, where

$$X = \frac{\sqrt{(3)}a}{2}\eta, \qquad Y = \frac{a}{2}\xi. \tag{46}$$

The load W will be considered in terms of the load per unit area q, where

$$q = \frac{2W}{\sqrt{(3)}a^2}. \tag{47}$$

In the case of the rectangular, pin-supported grillage considered in Section 4, it will be assumed that the overall dimensions of the rectangular boundary are A and B in the X and Y directions respectively, so that

$$A = \frac{\sqrt{(3)}an}{2}, \qquad B = \frac{am}{2}. \tag{48}$$

Then from equation (27) the distributed load per unit area, q, is given by

$$q = \sum_{r=1}^{n-1} \sum_{s=1}^{m-1} q_{rs} \sin\frac{\pi r}{A} X \sin\frac{\pi s}{B} Y \tag{49}$$

where

$$q_{rs} = \frac{2d'_{sr}}{\sqrt{(3)}a^2}.$$

In the expressions for K_5 to K_7 given by equations (19) to (21), μ and ν take the values $\pi sa/2B$ and $\sqrt{(3)}\pi ra/2A$ respectively, so that for any given values of r and s, μ and ν diminish as the fineness of the mesh increases. If then the powers of μ and ν higher than the fifth order can be ignored,

$$K_7 = \alpha[3\mu^2 + \nu^2]^2.$$

On substituting the above values into the expression for ω given by equation (31), this deflection becomes

$$\omega = \sum_{r=1}^{n-1} \sum_{s=1}^{m-1} \frac{q_{rs}}{\pi^4 D(r^2/A^2 + s^2/B^2)^2} \sin\frac{\pi r X}{A} \sin\frac{\pi s Y}{B} \tag{50}$$

where

$$D = \frac{3\sqrt{(3)}a^2\alpha}{8}. \tag{51}$$

It will be seen that equation (50) coincides with the solution for a pinned rectangular plate given by Navier (cf. [4], p. 109).

Applying the substitution given by equations (46) and (47) to the deflection of a triangular mesh grillage with clamped circular boundaries given by equation (35) yields

$$\omega = \frac{q}{64D}[R^2 - X^2 - Y^2]^2 \tag{52}$$

where D is given by equation (51). This corresponds to the solution for clamped circular plates (see [4], p. 55).

Again, making the same substitutions into the expression given by equation (45) for the deflection of a triangular mesh grillage with pinned triangular boundaries results in the expression

$$\omega = \frac{q}{64AD}[X^3 - 3Y^2X - A(X^2 + Y^2) + \tfrac{4}{27}A^3][\tfrac{4}{9}A^2 - a^2 - X^2 - Y^2] \tag{53}$$

where D is again given by equation (51). As the grillage becomes infinitely fine, a tends to zero and equation (53) then coincides with Woinowsky-Krieger's solution for a uniformly loaded pinned triangular plate (see [4], p. 313).

8. CONCLUDING REMARKS

It has been shown that finite difference methods may be extended to the analysis of triangular mesh grillages by the employment of oblique co-ordinates. The solutions presented here are particularly useful in the analysis of grillages with large numbers of members and can be employed to speed considerably both manual and computer methods of solution. All the solutions given in the paper lead to a value of D for the grillage stiffness given by equation (51). It would appear then that this value is a fundamental property of these grillages.

By arguments analogous to those applied to periodic meromorphic functions in the complex plane, it is possible to show that any regular grillage pattern can be subdivided into parallelogram modules. The behaviour of such grillages can then be described in terms of two finite difference operators for which a unit step is equal one side of the module. Thus, in theory, any regular grillage may be analysed by reference to an oblique co-ordinate system.

REFERENCES

[1] J. P. Ellington and H. McCallion, *Aeronaut. Q.* **VIII**, 360 (1957).
[2] Thein Wah, *Proc. Am. Soc. civ. Engrs* **90** (E.M.2), 83 (1964).
[3] J. D. Renton, *Int. J. mech. Sci.* **6**, 209 (1964).
[4] S. Timoshenko and S. Woinowsky-Krieger, *Theory of Plates and Shells.* McGraw-Hill (1959).

(*Received* 6 *July* 1965)

Résumé—Les équations de différence finie pour l'analyse des grillages à mailles triangulaires sont dérivées de l'hypothèse suivante: la rigidité de torsion des poutres individuelles est négligeable. Des solutions générales à ces équations sont indiquées et peuvent être utilisées comme moyen rapide, pour déterminer la flexion de ces grillages. Ces solutions sont appliquées pour trouver les flexions des grillages de périmètre rectangulaire, circulaire et triangulaire. Dans les cas particuliers qui sont étudiés ici, on voit que les grillages ont tendance à ses comporter comme des plaques, étant donné que la maille devient infiniment fine.

Zusammenfassung—Differenzen-Gleichungen für die Analyse von dreieckigen Gitter Schwellrosten sind von der Annahme abgeleitet das die Verdrehungssteifheiten der einzelnen Balken unbedeutend sind. Allgemeine Lösungen dieser Gleichungen sind gegeben und können als ein schnelles Hilfsmittel für die Auffindung von Durchbiegungen solcher Schwellroste verwendet werden. Diese Lösungen weden angewendet um die Durchbiegungen von Schwellrosten mit rechtwinkeligen, kreisförmigen und dreieckigen Begrenzungen zu geben. In besonders geprüften Fällen wird angezeigt das, wenn die Gitter unendlich fein werden, neigen die Schwellroste dazu, sich wie Platten zu verhalten.

Абстракт—Конечные уравнения разницы для анализа решёток треугольной сетки выведены на основании предположения, что жёсткость индивидуальных стержней при кручении—незначительна. Даны общие решения этих уравнений, и они могут применяться, как быстрый способ нахождения прогибов таких решёток. Эти решения применяются, чтобы дать прогибы решёток с прямоугольными, круглыми и треугольными контурами. В исследуемых особенных случаях показано, что, когда сетка станавится бесконечно мелкой, решётки склонны вести себя, как пластины.